nature neuroscience

# Motor modulation of afferent somatosensory circuits

SooHyun Lee[1,3], George E Carvell[2] & Daniel J Simons[1]

**A prominent feature of thalamocortical circuitry in sensory systems is the extensive and highly organized feedback projection from the cortex to the thalamic neurons that provide stimulus-specific input to the cortex. In lightly sedated rats, we found that focal enhancement of motor cortex activity facilitated sensory-evoked responses of topographically aligned neurons in primary somatosensory cortex, including antidromically identified corticothalamic cells; similar effects were observed in ventral posterior medial thalamus (VPm). In behaving rats, thalamic responses were normally smaller during whisking but larger when signal transmission in brainstem trigeminal nuclei was bypassed or altered. During voluntary movement, sensory activity may be globally suppressed in the brainstem, whereas signaling by cortically facilitated VPm neurons is simultaneously enhanced relative to other VPm neurons receiving no such facilitation.**



The somatosensory system intimately cooperates with the motor system during tactile exploration and active touch. In the whisker sensorimotor system of rats, extensive interconnections exist between sensory and motor neural subsystems[1]. During whisking, motor cortex activity is elevated[2], but sensory-evoked responses in the lemniscal system are typically attenuated[3–7].

Motor cortex projections to deep layers of primary somatosensory cortex (S1) can potentially excite corticothalamic cells either monosynaptically or by local circuit interactions[8,9]. S1 corticothalamic neurons are thus strategically positioned to regulate activity in thalamocortical circuits during voluntary movement[9]. Corticothalamic feedback can enhance thalamic firing and response tuning[10,11]. The circumstances in which corticothalamic neurons are engaged are not yet known. A substantial proportion of corticothalamic cells are weakly responsive or even silent in anesthetized[12,13] and awake animals[14–17].

We found that S1 corticothalamic neurons in whisker/barrel cortex responded more robustly to whisker deflections when motor cortex activity was focally enhanced. Similar effects were observed in topographically aligned thalamic neurons in the VPm. Thus, cortico-thalamo-cortical circuitry is engaged by other functionally related cortical centers. During whisking in behaving rats, VPm responses were suppressed when whisker follicles were stimulated but were enhanced when processing in brainstem nuclei was bypassed or experimentally altered. Corticothalamic feedback may provide context-dependent regulation of information processing in sensory thalamocortical circuits during active touch.

## RESULTS

### vFMCx activation effects on S1 corticothalamic neurons

We used multiple-barrel microelectrodes in lightly sedated rats to record and apply the $GABA_A$ receptor antagonist bicuculline methiodide (BMI) to the vibrissal region of the face area in primary motor cortex (vFMCx). Focal BMI application produced a spatially localized and reversible increase in vFMCx multi-unit activity (MUA; **Fig. 1**). MUA increased ~3.5-fold and recovered 30–60 min after termination of BMI injection (**Fig. 1a**,**b**). In one experiment, we simultaneously recorded MUA from four electrodes spaced ~500 μm apart in the tangential plane (**Fig. 1c**,**d**). At a site 500 μm removed from the BMI injection, MUA activity increased <0.5-fold compared with the application site (also see ref. 18).

We examined the effects of vFMCx BMI application on neurons in lower layer 5 and layer 6 (hereafter denoted as L-6) of S1 barrel cortex (**Supplementary Fig. 1** online). We found that 29 cells were located in a barrel-related column corresponding topographically to the BMI vFMCx site; 12 neurons were located in adjacent, nonaligned S1 columns. For aligned recordings (**Fig. 1e**), BMI in vFMCx increased spontaneous (control, 5.85 ± 1.70; BMI, 6.93 ± 2.36 Hz; $P = 0.03$, paired $t$ test) and whisker-evoked firing (stimulus onsets: control, 0.95 ± 0.52; BMI, 1.15 ± 0.65; spikes per stimulus, $P < 0.001$, paired $t$ test). We found no relationship between BMI-induced increases in vFMCx MUA firing rates and the magnitude of firing rate change in S1 neurons ($R^2 = 0.008$, $P = 0.66$). When vFMCx and S1 sites were nonaligned (**Fig. 1e**), we observed no consistent effect of motor cortex activation for spontaneous or whisker-evoked firing ($P > 0.05$, paired $t$ tests). Four non-aligned cells showed small, but statistically significant, firing increases or decreases ($P < 0.05$), but these were unrelated to S1 recording depth or to the depth of VFMCx BMI application.

For the aforementioned data, we simply recorded L-6 neurons that could be identified extracellularly; thus, the sampled population may have included corticothalamic and non-corticothalamic cells. We therefore examined a second sample comprised of antidromically identified S1 corticothalamic neurons. Because most S1 corticothalamic neurons project in topographic fashion to VPm[19], we aligned the S1 recording and VPm stimulating sites. We also aligned the BMI

[1]Department of Neurobiology, University of Pittsburgh School of Medicine, 200 Lothrop Street, Pittsburgh, Pennsylvania 15261, USA. [2]Department of Physical Therapy, University of Pittsburgh School of Health and Rehabilitation Sciences, 166 Atwood Street, Pittsburgh, Pennsylvania 15260, USA. [3]Present address: Smilow Neuroscience Program, New York University School of Medicine, 522 1st Avenue, New York, New York 10016, USA. Correspondence should be addressed to D.J.S. (cortex@pitt.edu).

Received 23 July; accepted 17 October; published online 16 November 2008; doi:10.1038/nn.2227

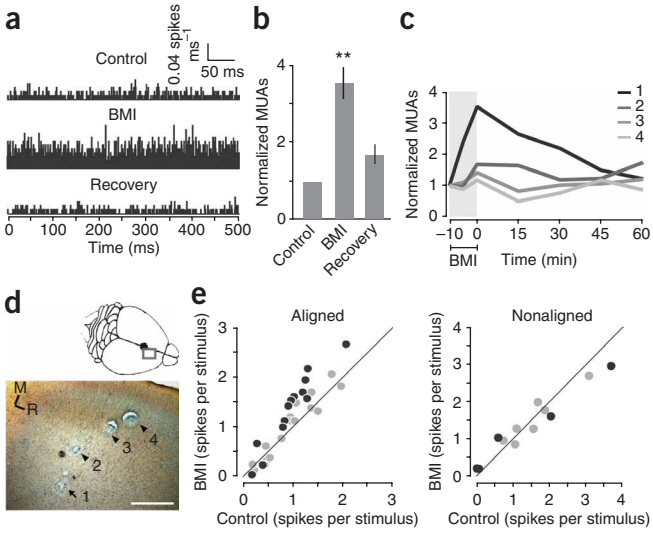


**Figure 1** The effect of BMI micro-iontophoresis on vFMCx and S1 L-6 neurons. (**a**) PSTHs show spontaneous MUA recorded from vFMCx during 80 500-ms epochs. Application of 10 mM BMI for 5 min caused an ~threefold increase in MUA. MUA returned to baseline within 30 min of cessation of BMI application. (**b**) MUA was normalized to activity during control conditions for 21 BMI applications in four experiments. Error bars indicate mean ± s.e.m. ** $P < 0.005$, paired $t$ test. (**c**) The spread of BMI's effect was evaluated by recording MUA simultaneously from four electrodes placed ~500 μm apart horizontally at a depth of 1,500 μm. One electrode delivered BMI (black solid line). BMI application for 10 min (gray area) increased MUA at the delivery site but minimally affected responses at other locations. (**d**) Histological localization of the recording sites. A small electrolytic lesion was made at each site (arrow and arrowheads). Numbers indicate the sites for data shown in **c**. Horizontal section (70 μm) was processed for cytochrome oxidase with thionin counterstain. Site 1 (full arrow) indicates the site of BMI application. Scale bar represents 500 μm. Inset, gray rectangle indicates the region shown in the photomicrograph and the dot represents the approximate location of bregma. (**e**) Effect of vFMCx activation on S1 L-6 neurons. ON response magnitudes for 29 topographically aligned and 12 nonaligned neurons were plotted for control and BMI conditions. Individual neurons showing a significant difference are indicated as closed circles ($P < 0.05$).

micro-iontophoresis microelectrode in vFMCx with the S1 (and VPm) site. We recorded 38 antidromically confirmed corticothalamic neurons at depths of 1,400–1,950 μm. Consistent with previous reports[12–15], most of the corticothalamic neurons (60%) were silent, showing no spontaneous activity or whisker-evoked responses. Axon conduction properties were similar to those described previously (**Supplementary Table 1** online). Similar to S1 corticothalamic cells in awake rabbits[14], neurons having faster axonal conduction velocities were more responsive to whisker deflection (linear regression, $P = 0.03$).

BMI activation of vFMCx enhanced the responsiveness of S1 corticothalamic neurons, in some cases leading to the appearance of whisker-evoked discharges in otherwise silent cells. An example corticothalamic neuron (**Fig. 2a**) fired only one spike for 80 whisker deflections in the control condition. During vFMCx BMI application, the cell responded more robustly to whisker movements (29 spikes).

We tested 38 corticothalamic neurons, of which 23 were silent in the control condition, having no spontaneous or whisker-evoked firing. During vFMCx activation, 19 of the 38 neurons showed changes in firing rate; the firing rate increased in all but one of these. Of the 19 unaffected corticothalamic neurons, 17 were silent in the control condition and remained so with vFMCx BMI application. Two persistently silent cells were tested with larger and longer duration BMI currents and both remained silent. On average, whisker-evoked ON responses were significantly increased during vFMCx activation for all 38 neurons (control versus BMI, mean ON 1.02 ± 1.11 versus 2.86 ± 2.97 spikes per 80 stimuli, $P = 0.02$, paired $t$ test; **Fig. 2b,c**). The total activity during the entire 500-ms trial, including the pre-stimulus spontaneous activity and plateau and OFF responses, also increased ($P = 0.004$, paired $t$ test). BMI vFMCx effects on S1 corticothalamic neurons were unrelated to S1 recording depth, conduction velocity or supernormality (see Methods).

### vFMCx activation effects on thalamic barreloid neurons

We examined whether vFMCx facilitation influences the responses of VPm neurons. An example cell, recorded in the physiologically defined B1 barreloid (**Fig. 3a**), showed increased ON responses to deflection of the B1 whisker (the principal whisker) when BMI was injected at a vFMCx site where row-B (second-most dorsal row) whisker movements were evoked before paralyzing the rat (1.49 versus 3.10 spikes per stimulus, $P = 0.02$, $t$ test). We then repositioned the recording electrode

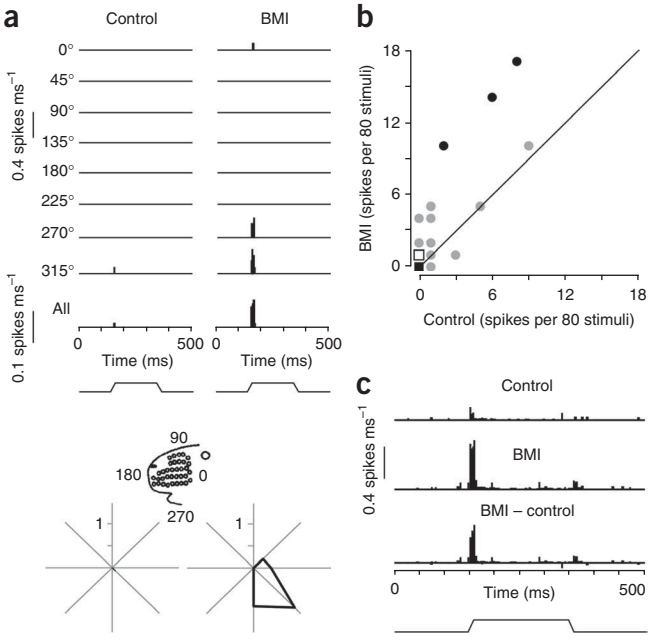


**Figure 2** Effects of vFMCx activation on antidromically identified corticothalamic neurons in S1. (**a**) PSTHs show accumulated responses of a corticothalamic neuron (recording depth, 1,680 μm) to principal whisker deflection before and during vFMCx activation by BMI micro-iontophoresis. The principal whisker was deflected ten times at eight different angles and the response accumulated over all of the angles is shown in the bottom PSTH. The vertical scale represents the spike probability per 1-ms bin. Stimulus waveform is indicated below. Polar plots illustrate responses to stimulus onsets in polar coordinates (spikes per stimulus). Inset indicates orientation with respect to the face. (**b**) vFMCx activation by BMI micro-iontophoresis increased principal whisker–evoked responses of topographically aligned corticothalamic neurons ($n = 38$). ON responses are spike counts during a 30-ms period following deflection onsets. Gray line denotes unity. Individual neurons showing a significant difference are indicated as closed circles ($P < 0.05$). Note that many data points near 0 are superimposed (circle, $n = 1$; closed square, $n = 19$; open square, $n = 5$) and that one data point ($x$, $y = 1$, 30) is not plotted to preserve clarity of the plot. (**c**) Population all-angle PSTHs were constructed from all corticothalamic neurons. Data are presented as in **a**.

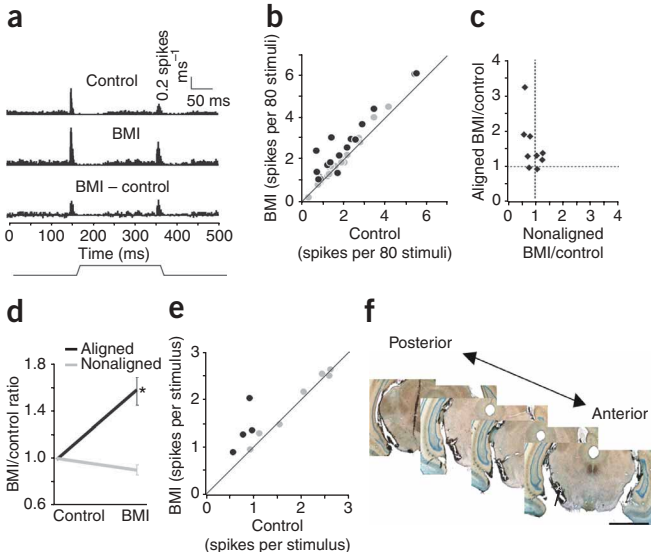


**Figure 3** The effect of vFMCx activation on VPm neurons. (**a**) PSTHs from a neuron in topographically aligned VPm. (**b**) Data from 36 neurons in aligned VPm. Individual neurons showing a significant difference in ON response are indicated as closed circles ($P < 0.05$). Data are presented as in **Figure 2b**. (**c**) Topographically specific effect of BMI application to vFMCx on thalamic barreloid neurons. Proportional changes in ON responses to principal whisker deflection by vFMCx BMI were compared in nine pairs of simultaneously recorded neurons from aligned and nonaligned VPm sites relative to vFMCx BMI site. Values >1.0 indicate VPm response facilitation during BMI condition. (**d**) Normalized VPm responses during vFMCx BMI application versus the control condition (* $P = 0.05$, paired $t$ test). (**e**) vFMCx affected VPm neurons after ablation of corticobulbar fibers. Multiple, small electrolytic lesions were produced in the right cerebral peduncle before recordings. The scatter plot shows the effects in 11 aligned neurons studied in two experiments. Individual neurons showing a significant difference ($P < 0.05$, paired $t$ test) are indicated as closed circles. Data are presented as in **Figure 2b**. (**f**) Photomicrographs of coronal sections through the caudal end of the diencephalon; arrow in lower section indicates damaged fiber tract in the right hemisphere (reversed in figure). Scale bar represents 3.0 mm.

into the physiologically defined D1 barreloid. BMI application at the same row-B vFMCx site failed to alter the thalamic cell's D1 whisker-evoked firing ($P > 0.05$, $t$ test). Principal whisker–evoked ON responses of 36 neurons in topographically aligned barreloids were larger during vFMCx activation (2.01 ± 0.62 versus 2.37 ± 0.69 spikes per stimulus, $P = 0.0001$, paired $t$ test; **Fig. 3b**). Nearly half (17) of the individual cells showed a significant increase. Mean spontaneous activity also increased ($P = 0.0001$), as did responses to stimulus offset ($P = 0.0003$) and plateau ($P < 0.0001$). We found no relationship between increased vFMCx MUA firing rates and changes in the VPm response ($R^2 = 0.03$, $P = 0.34$). When vFMCx BMI application and thalamic barreloid recording sites were not topographically aligned, vFMCx facilitation did not affect average spontaneous or whisker-evoked firing rates ($P > 0.05$, paired $t$ tests). Control ON responses in aligned and nonaligned neurons were equivalent ($P > 0.05$, $t$ test).

We further tested the topographic dependency of vFMCx effects by simultaneously recording nine pairs of VPm neurons. For each pair, one neuron was topographically aligned relative to the vFMCx BMI application site and the other was recorded in a physiologically defined barreloid at least one row removed (nonaligned). Paired recordings control for possible variability in BMI micro-iontophoresis and for possible changes in the momentary state of the brain during light sedation. In most pairs (**Fig. 3c**), responses increased in the aligned VPm neuron ($P < 0.05$, paired $t$ test), whereas only small or no changes occurred in the nonaligned cell ($P > 0.05$). ON responses of aligned neurons increased, whereas those of nonaligned neurons remained at control levels (BMI/control ratio, aligned versus nonaligned, 1.57 ± 0.35 versus 0.9 ± 0.13, $P = 0.05$, paired $t$ test; **Fig. 3d**). BMI-induced increases in aligned neuron–evoked firing were similar to those observed for the nonpaired recordings ($P > 0.05$, $t$ test).

vFMCx facilitation effects on VPm neurons could be mediated by S1 corticothalamic neurons; this is consistent with the finding that BMI effects were more robust for S1 than for VPm neurons. The effects that were observed in the thalamus could also reflect more indirect, corticobulbar influences on brainstem centers that relay afferent activity to VPm. Therefore, we ablated corticobulbar fibers in the crus cerebri and similarly tested 11 neurons in two experiments (see Methods; **Fig. 3e**,**f**)[18]. vFMCx facilitation enhanced the firing rates of thalamic neurons (control versus BMI, ON 1.50 ± 0.38 versus 1.73 ± 0.32 spikes per stimulus, $P = 0.05$, paired $t$ test). To ensure that the lesion itself did not alter VPm responses, we compared pre-BMI ON responses from corticobulbar-ablated animals to those obtained in intact animals and found that they were equivalent ($P > 0.05$, $t$ test). We conclude that enhanced vFMCx activity increases the spontaneous and whisker-evoked firing of topographically aligned VPm neurons. Although the corticobulbar ablation manipulation is not by itself conclusive, the topographic nature of the findings is consistent with a S1 corticothalamic neuron–mediated effect (see Discussion).

### Whisker follicle stimulation and whisking

We next examined whether afferent-evoked responses in VPm are modulated during voluntary whisking when motor cortex is probably active[2]. We recorded VPm local field potentials (LFPs) and MUA in freely behaving rats, and compared sensory-evoked responses during periods of exploratory whisking and periods of alert wakefulness in the absence of whisking (that is, nonwhisking). In both conditions, whiskers did not contact objects in the testing apparatus.

For controlled sensory input, we applied brief electrical stimuli to a single whisker follicle (**Supplementary Fig. 2** online). Such stimulation evoked a pronounced negative LFP peak in topographically aligned VPm (**Supplementary Fig. 3** online). The LFP was similar in timing and shape to the LFPs recorded in VPm of sedated rats in response to whisker deflections[20]. Brief periods (several hundred microseconds) of short-latency, synchronous thalamic population spiking occurred during negative inflections of the LFP waveform; the slope of the initial negativity and the timing of the immediately following second negativity, occurring <1 ms later, were highly correlated with stimulus strength (for example, deflection velocity[20]). Electrical stimulation of the follicle (or medial lemniscus, below) evoked highly synchronous afferent activity and especially steep inflections in the thalamic LFP. Example LFPs (**Fig. 4a**) were taken from a single recording session that consisted of 175 stimulus presentations during whisking and 211 during nonwhisking. Stimulus-evoked responses were significantly smaller during whisking (43.64 ± 13.63 versus 52.04 ± 18.18 μV, $P = 0.004$, Mann-Whitney test). We obtained similar results for MUA (**Fig. 4b**); as in the case of whisker deflection, the greatest MUA activity occurred during the first two negative inflections of the LFP. Because of the highly transient nature of the response evoked by the electrical stimulus, we calculated MUA during a 1-ms window starting ~2.5 ms after the whisker follicle stimulus. For the single session recordings (**Fig. 4b**), whisker follicle stimulation evoked fewer spikes during whisking (0.13 ± 0.17 versus 0.24 ± 0.21 spikes per stimulus, $P = 0.002$, Mann-Whitney test).

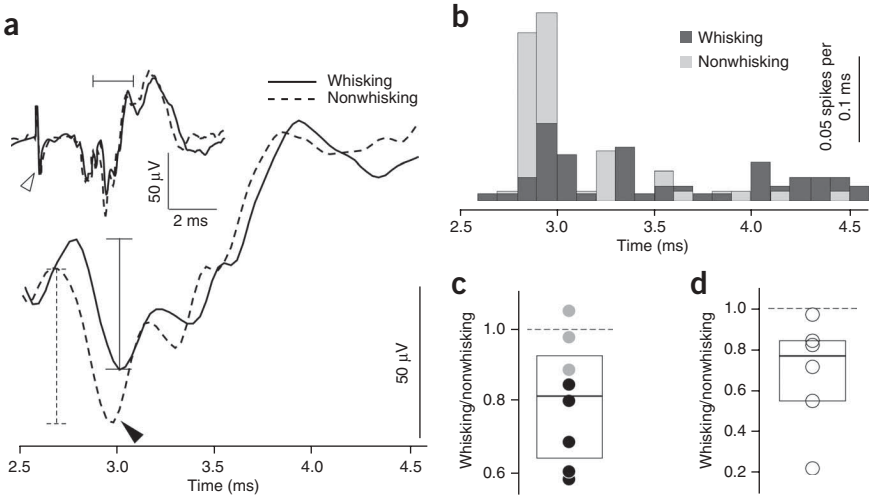


**Figure 4** Whisker follicle stimulation–evoked VPm LFPs during whisking and nonwhisking conditions. (**a**) The evoked LFP was larger during nonwhisking than during whisking; the LFP was averaged from 175 whisking and 211 nonwhisking whisker follicle stimuli. Solid arrowhead in nonwhisking trace denotes peak LFP negativity. Verticals lines indicate peak LFP amplitudes. Inset shows full traces including stimulus artifact (open arrowhead) and the evoked LFP. The evoked LFPs in the inset (indicated by a horizontal bar) are shown at an expanded scale below. (**b**) PSTHs of simultaneously recorded MUA (0.1-ms bins). Whisker follicle stimulation evoked fewer spikes during whisking periods. LFP traces in **a** and PSTHs in **b** are temporally aligned. MUA spike counts were measured during a 1-ms window starting 2.5 ms after the whisker follicle stimulus. (**c**) Whisker follicle stimulation–evoked LFPs ($n = 8$ sessions). Peak-to-peak LFP amplitudes during whisking were normalized to values during nonwhisking ($P = 0.02$, Wilcoxon signed-rank test). The box plots indicate 25–75 percentile range and the line in the box indicates median. Data from each recording session in which there was a significant difference between whisking and nonwhisking are indicated as closed circles ($P < 0.05$, Mann-Whitney tests). (**d**) Whisker follicle stimulation–evoked MUAs ($n = 6$ sessions). Evoked spikes were normalized to values during nonwhisking ($P = 0.03$, Wilcoxon signed-rank test). Data are presented as in **c**.

We recorded thalamic LFPs in eight behavioral sessions from three rats (**Fig. 4c**). During whisking, whisker follicle stimulation evoked smaller responses ($P = 0.02$, Wilcoxon signed-rank test). On average, response magnitudes were reduced by 20% (**Fig. 4c**). We also analyzed data from each recording session separately. Five of the eight datasets showed significantly smaller responses during whisking ($P < 0.05$, Mann-Whitney tests). At least one recording session in each of the three animals showed a statistically significant reduction. For MUA ($n = 6$ sessions; **Fig. 4d**), firing rates were lower during whisking ($0.19 \pm 0.08$ versus $0.28 \pm 0.10$ spikes, $P = 0.06$, Mann-Whitney tests). Effects were more robust when spontaneous firing rates were subtracted ($0.17 \pm 0.07$ versus $0.27 \pm 0.10$, $P = 0.03$); spontaneous MUA was slightly higher during whisking ($25.41 \pm 13.92$ versus $13.47 \pm 5.00$ Hz, $P = 0.16$).

## Medial lemniscus stimulation and whisking

Pharmacologically elevated vFMCx activity enhances VPm firing. In behaving rats, however, we observed diminished VPm responses during whisking. This reduction could reflect smaller neuronal responses in the trigeminal principal sensory nucleus (PrV), the main afferent relay to VPm. To evaluate possible corticobulbar contributions to the observed VPm response, we bypassed brainstem processing by directly stimulating trigeminothalamic axons in the medial lemniscus. Localized LFP responses were evoked in VPm by electrical microstimulation delivered via a microelectrode placed in a physiologically corresponding location in medial lemniscus (**Supplementary Fig. 3**).

LFPs from an example recording session show two pronounced negative waves, an initial peak occurring ~0.8 ms after medial lemniscus stimulation and a second peak occurring ~2 ms later (**Fig. 5a**). We denote these two peaks as 'early' and 'late' components, respectively. Note that whisker follicle stimulation evoked only one large negative peak, corresponding to the 'early' component of the medial lemniscus–evoked response. The later medial lemniscus–evoked component probably reflects a secondary VPm discharge occurring at the termination of the refractory period of the thalamic cells (**Supplementary Fig. 4** online). Both early and late components of the medial lemniscus–evoked LFP response were significantly larger during whisking (early, $126.3 \pm 20$ versus $60.25 \pm 15$ μV, $P = 0.0001$; late, $217.5 \pm 32.5$ μV versus $157.5 \pm 40$, $P = 0.0001$, Mann-Whitney tests; **Fig. 5a**). The beginning of the thalamic spiking response was typically obscured

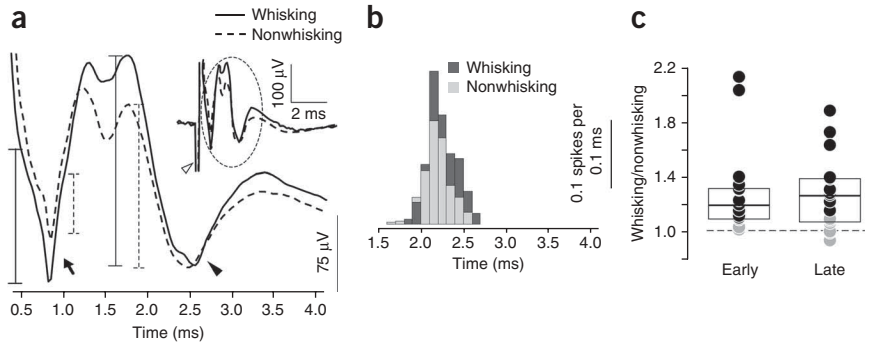


**Figure 5** Medial lemniscal stimulation–evoked VPm LFPs. (**a**) Evoked LFPs, both early and late components, were larger during whisking than during nonwhisking; arrow indicates early and solid arrowhead indicates late negativities. LFPs were determined on the basis of 379 nonwhisking and 207 whisking stimuli. Inset shows full traces, including stimulus artifact (open arrowhead) and evoked responses (dashed ellipse). (**b**) PSTHs of simultaneously recorded MUA (0.1-ms bins). Because the beginning of the thalamic spiking response was obscured by the stimulus artifact, MUA spike counts were taken only during the late-response component, corresponding to the second positive-to-negative slope. Data are presented as in **Figure 4b**. (**c**) Medial lemniscus stimulation evoked proportionally larger early and late VPm responses during whisking ($P < 0.005$, Wilcoxon signed-rank tests). LFP amplitudes during whisking were normalized to those during nonwhisking. Data are presented as in **Figure 4c**.

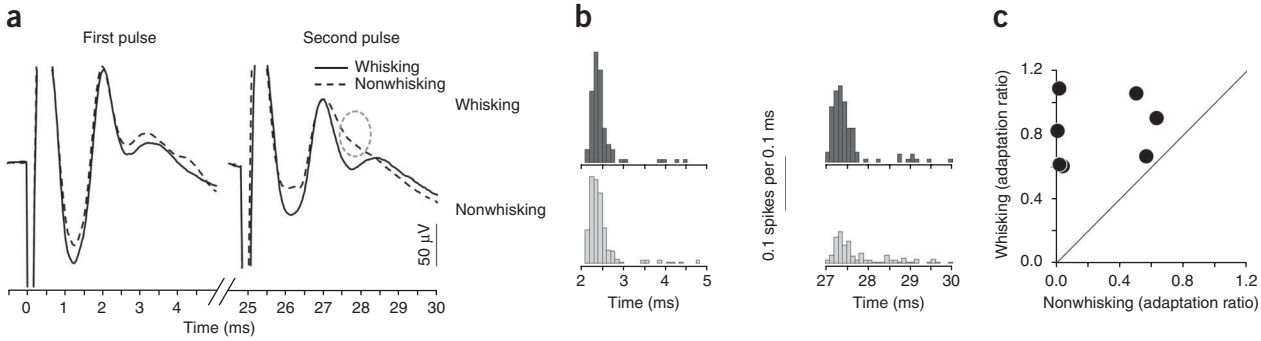


**Figure 6** Paired-pulse medial lemniscal stimulation. (**a**) LFP was larger during whisking ($P < 0.0005$, Mann-Whitney test; whisking, $n = 207$ stimuli; nonwhisking, $n = 417$). Paired-pulse suppression (25-ms interval) was less robust during whisking. Note that the late response to the second pulse was barely detectable during nonwhisking (dashed ellipse). (**b**) PSTHs of simultaneously recorded MUA (0.1-ms bins). Spike counts were larger during whisking in response to the second stimulus, and there was less paired-pulse suppression. Data are presented as in **Figure 4b**. (**c**) Adaptation of thalamic responses to paired-pulse medial lemniscus stimulation during whisking and nonwhisking periods. Paired-pulse adaptation indices for seven recording sessions are calculated as the ratio of MUA spikes counts evoked by the second pulse to those evoked by the first pulse. The gray line indicates the unity line.

by the stimulus artifact. We therefore analyzed MUA only during the late-response component, corresponding to the second positive-to-negative slope of the LFP. Medial lemniscus stimulation evoked more MUA spikes during whisking (late component, 0.80 ± 0.22 versus 0.54 ± 0.25 spikes per stimulus, $P < 0.0001$, Mann-Whitney test; **Fig. 5b**).

We normalized peak LFP amplitudes (17 sessions, 2 rats) obtained during whisking to those recorded during nonwhisking (**Fig. 5c**). Both early ($P < 0.0001$, Wilcoxon signed-rank test) and late ($P = 0.001$) component responses increased during whisking. We found statistically significant increases in 12 of the individual sessions ($P < 0.005$, Mann-Whitney test).

Although medial lemniscus stimulation bypasses the brainstem, brainstem firing could still affect the medial lemniscus–evoked response in VPm. If overall spiking is reduced in PrV during whisking, trigeminothalamic synapses might be less depressed, and medial lemniscus–evoked synaptic responses in VPm might therefore be larger. We therefore employed paired-pulse medial lemniscus stimulation under the assumption that the first pulse activates most of the medial lemniscus fibers terminating on VPm cells near the recording microelectrode. The second pulse, delivered 25 ms later, will occur when trigeminothalamic synapses are near-maximally, or at least substantially, depressed[21]. Thus, whisking versus nonwhisking differences in the VPm response to the second medial lemniscus pulse would probably be the result of effects other than trigeminothalamic synaptic depression or activity-related mechanisms in the brainstem.

Medial lemniscus–evoked LFP magnitudes were larger during whisking, and this was the case both for early- and late-response components and for first- and second-pulse responses (**Fig. 6**). During nonwhisking, the late LFP component of the second-pulse response was so small that it was barely detectable. Because these small LFP responses were difficult to quantify, we analyzed paired-pulse data using MUA. In one example (**Fig. 6b**), the second medial lemniscus pulse evoked fourfold more spikes during whisking than during nonwhisking (0.45 ± 0.08 versus 0.11 ± 0.07 spikes per stimulus, $P < 0.0001$, Wilcoxon signed-rank test); in this example, first-pulse spike counts did not differ between whisking and nonwhisking conditions. For seven recording sessions in two rats, the response to the second pulse was ~50% of that of the first response during nonwhisking (first versus second pulse; 0.64 ± 0.26 versus 0.29 ± 0.25 spikes per stimulus, $P < 0.0001$, Wilcoxon signed-rank test), whereas first- and second-pulse spike counts were equivalent during whisking (0.67 ± 0.26 versus 0.69 ± 0.28 spikes per stimulus, $P > 0.05$, Wilcoxon signed-rank test). The relatively larger second-pulse response during whisking may reflect facilitation of VPm neurons by motor-enhanced firing of corticothalamic cells evoked by the first pulse.

For the seven datasets, paired-pulse (adaptation) ratios were significantly smaller during nonwhisking, indicating stronger paired-pulse suppression (0.25 ± 0.15 versus 0.82 ± 0.10, $P = 0.003$, Wilcoxon signed-rank test; **Fig. 6c**); significant effects were observed in both animals. In four sessions, adaptation during nonwhisking was so robust that the second pulse evoked virtually no spikes (**Fig. 6c**). Paired-pulse suppression is also stronger during nonwhisking with infraorbital nerve stimulation[3].

We confirmed the observed differences in whisker follicle and medial lemniscus effects by testing a rat in which we implanted both whisker follicle– and medial lemniscus–stimulating wires. During individual recording sessions, whisker follicle and medial lemniscus stimuli were interleaved in pseudorandom blocks. During whisking, whisker follicle stimulation evoked smaller LFP responses (11.56 ± 12.89 versus 20 ± 13.33 μV, $P = 0.02$, Mann-Whitney test; **Fig. 7a**), whereas medial lemniscus stimulation evoked larger ones in the same recording session

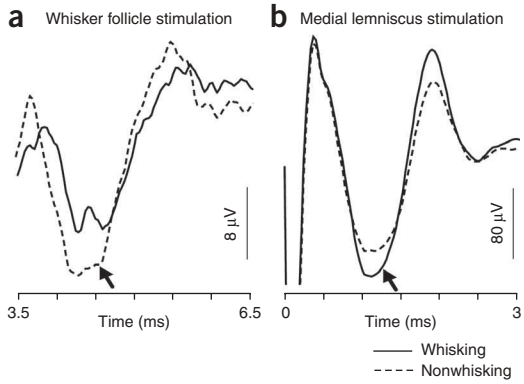


**Figure 7** Contrasting effects of whisker follicle and medial lemniscus stimulation in the same animal. (**a**,**b**) VPm LFPs evoked by interleaved (**a**) whisker follicle stimulation and (**b**) medial lemniscus stimulation in one animal during a single recording session. Whisker follicle stimulation evoked a smaller response during whisking, whereas medial lemniscus stimulation evoked a larger response. Arrows indicate evoked LFP negativity.

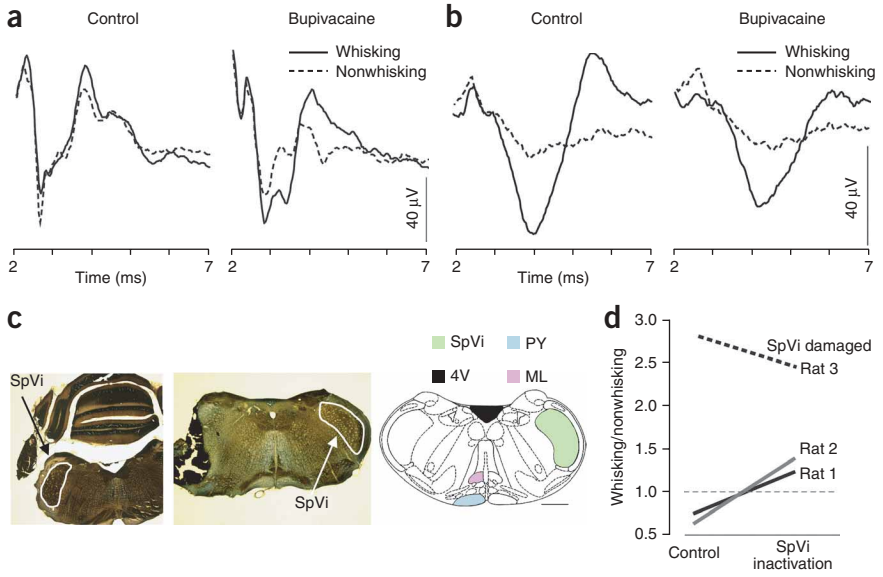


**Figure 8** Whisker follicle stimulation evokes larger VPm responses during whisking when SpVi is inactivated. (**a**) When SpVi was inactivated by bupivacaine infusion, the response to whisker follicle stimulation during whisking was larger than during nonwhisking, the converse of the control condition. (**b**) Damage to SpVi resulted in a larger whisker follicle–evoked VPm during whisking than during nonwhisking, regardless of infusion of bupivacaine into SpVi. (**c**) Photomicrographs of coronal sections through SpVi, demarcated by white lines. Arrow indicates histological localization of the implanted cannula (left). Severe damage to SpVi by the implanted cannula is evident in the middle section. The line drawing shows the location of SpVi at 13.24 mm posterior to bregma. Scale bar represents 1 mm and applies to all three images. 4V, fourth ventricle; ML, medial lemniscus; Py, pyramidal tract. (**d**) Larger VPm responses to whisker follicle stimulation were observed during whisking in SpVi-inactivated or SpVi-damaged rats. Peak of LFP during whisking was normalized to the peak LFP during nonwhisking for each recording session. The gray dotted line at 1.0 indicates no changes.

(214.20 ± 14.89 versus 181.1 ± 32.44 μV, $P = 0.0007$, Mann-Whitney test; **Fig. 7b**). Thus, differences in VPm responses during whisking and nonwhisking depend critically on the involvement of brainstem components of the trigeminothalamic system.

### Inactivation of SpVi

PrV contains few, if any, inhibitory interneuron but does receive inhibitory projections from the interpolaris subdivision of the spinal trigeminal complex (SpVi)[22,23]. Such inhibitory circuitry may be responsible for whisking-related suppression observed in VPm with whisker follicle stimulation. In three rats, we pharmacologically inactivated SpVi. Whisker follicle–evoked thalamic LFPs recorded during one session were smaller during whisking (49.2 ± 20 versus 65.8 ± 20 μV, $P < 0.0001$, Mann-Whitney test; example shown in **Fig. 8a**). Infusion of a sodium channel blocker, bupivacaine, in SpVi reversed the whisking effects; that is, evoked LFPs were now larger during whisking (72 ± 20 versus 58 ± 20 μV, $P = 0.0001$, Mann-Whitney test). Comparable results were observed in a second rat (**Fig. 8**). Thus, during SpVi inactivation, whisker follicle stimulation effects were similar to those obtained during medial lemniscus stimulation in otherwise intact rats.

A third rat showed whisker follicle–evoked VPm responses that were larger during whisking than even those obtained in the control condition (50 ± 28 versus 20 ± 14 μV, $P < 0.0001$, Mann-Whitney test; **Fig. 8b**); subsequent bupivacaine infusion had no effect (42 ± 24 versus 16 ± 16 μV, $P < 0.0001$, Mann-Whitney test; **Fig. 8b**). Histology revealed extensive damage to SpVi by the cannula itself, which was found to have penetrated deep in the nucleus (**Fig. 8c**).

Taken together, our results suggest that the whisking-related suppression that we observed in VPm following whisker follicle stimulation occurs at the level of the brainstem. Facilitation effects observed with medial lemniscus stimulation, when the brainstem is bypassed, probably reflect unmasked corticothalamic feedback.

## DISCUSSION

We investigated motor modulation of afferent activity in the whisker-to-barrel pathway, the trigeminal discriminative touch homolog of the dorsal column/medial lemniscal system. During whisking, vFMCx activity is tonically elevated[2], probably engaging brainstem pattern generating circuits[24,25]. We found that focal, pharmacological enhancement of firing in deep layers of motor cortex facilitated whisker-evoked responses in both topographically aligned S1 corticothalamic neurons and VPm neurons. During voluntary whisking, VPm responses were smaller when sensory transmission was intact but were larger when signal processing in brainstem trigeminal nuclei was bypassed or experimentally altered. Our results using whisker follicle microstimulation confirm findings obtained with infra-orbital nerve stimulation[3].

Corticothalamic synapses comprise almost half of the synaptic input to thalamic neurons and are more numerous than synapses from ascending fibers[26–28]. Inactivation of S1 alters thalamic receptive fields[29,30] and reduces evoked thalamic responses[31,32]. Conversely, focal enhancement of S1 L-6 activity facilitates neuronal responses in the topographically aligned area in VPm and suppresses responses in adjacent, nonaligned areas[18]. Notably, many corticothalamic cells are only weakly peripherally driven or are altogether silent, even in awake animals[12–17]. Limited responsiveness seems incongruous with anatomical findings that corticothalamic cells reside in an infragranular thalamo-recipient zone[19] and that many receive monosynaptic thalamic inputs[33]. Infragranular laminae also receive substantial projections from deep layers of motor cortex[8,9]. Our results indicate that inputs to S1 from another functionally related cortical area influence the excitability of corticothalamic neurons.

Focal pharmacological enhancement of motor cortex facilitated topographically aligned corticothalamic cells in barrel cortex and VPm. The latter effects may have been mediated by S1 corticothalamic cells, which are known to project to VPm barreloids in a topographic fashion[19]. A role for S1 corticothalamic neurons could potentially be established directly by inactivating sensory cortex. Cortical inactivation, however, could induce burst-mode thalamic firing unless carefully titrated[34], making it difficult to interpret small changes, or lack thereof, in VPm responses. A corticothalamic-mediated effect on VPm is consistent with our finding that facilitation was observed after the occurrence of crus cerebri lesions that probably eliminated potential corticobulbar effects on brainstem relays. Direct stimulation of medial lemniscus fibers, which bypasses the brainstem, evoked larger VPm responses during whisking. With paired-pulse stimulation, relative increases in the VPm response were even larger for the second pulse. We attribute this increase to facilitation by recurrent excitatory

corticothalamic activity that was evoked by the first pulse. Consistent with these facilitating corticothalamic effects, medial lemniscus–evoked thalamic responses are diminished during widespread cortical inactivation[31,32]. Corticothalamic neurons in other cortical areas, such as S2 and nearby regions of parietal cortex, could also influence VPm cells, although fine-grained topographic specificity of these corticothalamic systems has not been described. Except for sparse projections to the dorsal-most part of VPm, motor cortex does not project to barreloids[1]. VPm neurons near the posterior nucleus border can be affected by electrical stimulation of motor cortex, however, by means of VPm cell dendrites that extend into a motor cortex projection zone in posterior nucleus[34]. It is not known whether such projections are topographic or are able to mediate the effects we observed using BMI micro-iontophoresis.

Descending motor commands are thought to engage local inhibition in second-order relay stations. Sensory transmission in the cuneate nucleus is suppressed during limb movements as a result of corticobulbar projections[35,36], and cutaneous inputs during active wrist movements are presynaptically inhibited in the spinal cord[37]. In the whisker-to-barrel system, whisking-related suppression probably occurs in PrV, mediated by inhibitory projections from SpVi[23,38]. When SpVi was inactivated, whisker follicle-evoked thalamic responses were enhanced, not suppressed, during whisking. Reduced brainstem transmission may disproportionately suppress relatively weak and unintended or potentially confusing sensory signals produced by movement of peripheral tissues. For fore- and hindlimbs, such signals might arise during incidental contact of the skin surface with nearby objects. Similar signal-to-noise enhancement may be advantageous in the whisker system, as trigeminal ganglion cells are active during whisking in air, although at rates that are approximately an order of magnitude smaller than those associated with direct object contact[39]. In contrast, information about whisker movement *per se* may be actively extracted via motor cortex modulation of the paralemniscal system[1,40].

We applied BMI focally in a region of motor cortex that has previously been found to be tonically active during whisking[2]. Repositioning the BMI electrode $<1$ mm alters its effects in both S1 and VPm. This finding is consistent with intracortical microstimulation studies of vibrissal motor cortex that showed some, albeit coarse, functional topography in that region[41,42]. This area of motor cortex, which we have referred to as vFMCx, is a component of a larger, integrated face representation in the primary motor cortex map[43]. Brief, low-threshold electrical stimuli produced small, discrete retractions of 2–3 neighboring whiskers, whereas larger stimulating currents evoked more generalized facial movements. Stimulation of a second, perhaps more specialized area of nearby motor cortex can produce rhythmic whisker protractions and retractions[44].

Our data suggest that cortical activity associated with whisking motor commands enhances sensory transmission in the thalamus. Results of the acute experiments suggest that such effects are highly topographic. On the other hand, available evidence indicates that peripheral tactile signals are attenuated in the brainstem. This is often referred to as motor-related gating. Thus, during active touch, sensory signaling in the lemniscal system may be globally diminished early at brainstem levels[23]. Simultaneously, activity in specific thalamocortical microcircuits may be facilitated in a context-dependent manner by S1 corticothalamic neurons (**Supplementary Fig. 5** online). Although VPm firing is reduced overall[3], signaling by the cortically facilitated neurons would be enhanced relative to other thalamic cells receiving no such facilitation.

The function of primary motor cortex is still in question[45], and use of different intracortical microstimulation parameters has led to different interpretations of the nature of motor maps[46]. Voluntary whisking is but one component of a constellation of complexly integrated sensorimotor behaviors involving the face, neck and respiratory muscles[47–49]. Notably, whisking occurs in relation to coordinated head movements. Motor commands from the face/head area of motor cortex, including vFMCx, could indirectly facilitate activity in subpopulations of VPm neurons depending, for example, on whether the animal is turning its head and orienting its whisker field toward a ventrally versus a dorsally located object. During voluntary whisking, sensory transmission in thalamocortical circuits may be modulated according to specific activation patterns that are generated in the motor map.

## METHODS

**Surgical procedures.** Data were collected from adult, 200–350-g female rats (Sprague-Dawley strain, Hill Top). Rats, anesthetized with halothane or isoflurane, were prepared for electrophysiological recordings[50]. After motor cortex mapping (below), animals were maintained under light narcosis (fentanyl, $\sim$10 μg per kg of body weight per h), artificially respired and immobilized by neuromuscular blockade. The rats' conditions were monitored by a computer program that continually assessed electroencephalogram, mean arterial pressure, arterial pulse rate and tracheal airway pressure waveform. Experiments were terminated if any of the above indicators could not be maintained in normal physiological ranges. All procedures involving rats were approved by the University of Pittsburgh Institutional Animal Care and Use Committee.

**Motor mapping.** We mapped motor cortex under isoflurane and before initiation of neuromuscular blockade. Whisker movements were evoked using intracortical microstimulation delivered through stainless steel microelectrodes (100–500 kΩ at 1 kHz). We delivered 30-ms trains of pulses (0.2-ms duration) at 300 Hz at a depth of 1,400–1,600 μm while observing whisker movements using a stereo microscope. We reduced current intensity to levels that evoked small ($\sim$1 mm) retractive movements of 1–3 neighboring whiskers; movements were reliably evoked, depending in part on anesthetic depth, with currents (50–200 μA) that were $\sim$1.5-fold larger than the threshold. Near-threshold microstimulation using such brief pulse trains produce retractive movements of contiguous whiskers, typically in the same whisker row[41,42]. Vibrissa movements were reliably evoked in a region 1–3 mm lateral from midline and 1–3 mm anterior to bregma. This region is part of a large face area in primary motor cortex as defined previously by others[43,44]. The general topographic organization of the whisker rows (row A, anteromedial; row E, posterolateral) was similar to that reported earlier[41,42].

In two experiments, we ablated corticobulbar fibers[18]. Before initiating neuromuscular blockade, face-related sites in the crus cerebri near the caudal diencephalon were identified using low-intensity microstimulation to evoke contractions of facial muscles. We made a series of small electrolytic lesions bracketing this region ventromedially and dorsolaterally.

**BMI micro-iontophoresis.** During acute recording sessions with fentanyl sedation and paralysis, motor cortical activity was enhanced by micro-iontophoretic application of BMI[18]. We used three- or seven-barrel glass microelectrodes, lowered to a depth of 1,400–1,600 μm, to apply BMI and to record MUA for monitoring BMI effects. Positive current (15–30 nA) was used to expel BMI; one or two barrels were used and BMI in the remaining reserve barrels was retained with negative current. In most cases, 5–10 min of BMI application induced reproducible and reversible changes in spontaneous activity. Positive current was subsequently maintained during whisker stimulation protocols, which lasted $\sim$5 min. Immediately thereafter, current polarity was reversed for BMI retention. Typically, a 40–60-min recovery period was sufficient for MUA to return to baseline. During an experiment, BMI was injected no more than 4–8 times. For each application, the microelectrode was relocated $\sim$100 μm up or down in the same penetration or a new penetration was made.

**Electrophysiological recordings.** Extracellular single-unit recordings were obtained from infragranular barrel cortex neurons (depths of 1,400–1,800 μm)

using 3 M NaCl-filled glass micropipettes (~1-μm tip diameter, 5–10 MΩ impedance at 135 Hz), similar impedance stainless steel microelectrodes or microelectrodes that were made from pulled and beveled quartz-insulated platinum-tungsten (90/10%) fibers. Recordings were targeted deep to layer 4 barrel centers, determined by prior physiologic mapping, as VPm-projecting corticothalamic neurons are preferentially located there[19]. Analog signals were amplified, bandpass-filtered at 0.3 –10 kHz and digitized at 32 kHz. Units were identified by spike amplitude and waveform criteria. If multiple units were present, only the largest amplitude unit was selected. Units were further isolated off-line using custom spike-sorting software. In two experiments, an Ekhorn-type microelectrode array (Thomas Recording) was used to record simultaneously in two separate thalamic barreloids.

**Whisker stimulation and data analysis.** A hand-held probe was used to identify the whisker that most effectively evoked activity (that is, the cell's principal whisker). The principal whisker was subsequently deflected using a piezoelectric stimulator that was attached 10 mm along the whisker hair. Ramp-and-hold stimulus waveforms were similar to those employed previously[50]. Whisker deflections, delivered at 1.5-s intervals, were applied ten times in each of eight directions that differed by 45° increments ($n = 80$ stimuli). Deflections were 1-mm displacements of 200-ms duration, with average onset and offset velocities of ~125 mm $s^{-1}$. Deflection angles were varied in pseudorandom order.

Unit responses were compiled into peri-stimulus time histograms (PSTHs) with 1-ms bins and quantified as the average number of spikes per stimulus during selected epochs. Responses to stimulus onsets (ON) and offsets (OFF) were computed during a 30-ms period after the beginning of whisker movement away from or back to its resting position. Spontaneous activity was measured during a 100-ms period before stimulus onset. Plateau responses were computed for a 100-ms period between onset and offset. Graphical results are shown as means ± s.e.m. Statistical analyses of spike counts were made using paired *t* tests, unless otherwise noted.

On termination of the experiment, the rat was deeply anesthetized with pentobarbital sodium (Nembutal, 100 mg per kg) and perfused transcardially for cytochrome oxidase histochemistry with Nissl staining. For verification of recording and stimulation sites, the barrel cortex was cut tangentially, whereas vFMCx and VPm were sectioned coronally (70-μm sections).

**Antidromic stimulation.** Electrical stimuli were applied to the topographically aligned site in VPm[13]. S1 corticothalamic cells were identified by constant latency (<0.1-ms jitter) at suprathreshold stimulation and by a refractory period of ≤2 ms. We also noted the presence or absence of a supernormal conduction period, which was defined as an increase in conduction velocity in response to the second of two pulses spaced <10 ms apart. Supernormality was calculated as the percent change in antidromic latency. If the neuron fired spontaneously, a collision test was performed (**Supplementary Fig. 6** online).

**Surgical procedure for recordings from behaving animals.** Rats underwent aseptic surgeries under isoflurane anesthesia. An insulated platinum-iridium wire (0.8–3 MΩ at 1,000 Hz) was slowly advanced into VPm while a hand-held probe was used to identify units that responded to a caudal whisker (for example, D2). Depending on the experiment, a stainless steel stimulating microelectrode (0.2–0.5 MΩ at 1,000 Hz) was also implanted in the trigeminothalamic portion of the medial lemniscus (6.0 mm posterior to bregma, 1.2 mm lateral to midline). Using physiological mapping of whisker-evoked medial lemniscus responses, we topographically aligned the medial lemniscus electrode with the VPm recording electrode. We used fixed implantation, as the experiments required that whisker follicle and/or medial lemniscus stimulation sites be topographically aligned with the VPm electrode.

Several days later, whisker follicle–stimulating wires and EMG recording wires were implanted in the face. For stimulating a single whisker follicle, we tunneled a pair of Teflon-coated stainless steel 0.003-inch wires under the skin to the mystacial pad contralateral to the VPm recording site (**Supplementary Fig. 2**). To monitor whisking electrophysiologically, we inserted EMG electrodes into the opposite mystacial pad. This was placed ipsilateral to the VPM recording site to avoid interference with the whisker follicle–stimulating wire.

**Behavior.** Rats were trained to stand on a small (5 × 7.5 cm) elevated platform that was 34 cm in height. A T-shaped bar of similar width was placed in front of the platform at the same height. Rats were trained to hold this T-shaped bar with the forepaws by leaning forward. This position ensured that the animal remained alert and that its whiskers did not contact any objects; thus, during the experiments, animals 'whisked-in-air'. Rats were water-deprived between daily experimental sessions. At trial onset, a plastic tube for delivering sweetened water was moved close to the animals' faces but did not touch them or the whiskers. Rats searched for the tube by whisking; after several seconds of searching/whisking, the animal was allowed to contact the tube and receive a water reward. The animal's behavior was recorded videographically. VPm and EMG activity were recorded on the audio tracks of the VHS tape. Off-line, video and EMG recordings (**Supplementary Fig. 7** online) were examined to identify periods of sustained whisking and nonwhisking. The mean length of whisking epochs was 2.63 ± 2.31 s (s.d.), and the mean inter-epoch interval, when the animal was not whisking, was 6.38 ± 4.30 s (**Supplementary Fig. 8** online).

**Afferent stimulation.** Whisker-follicle stimulation was produced with a Grass physiological stimulator and constant-current isolator. Stimuli consisted of 1 Hz cathodal 200–800-μA pulses of 0.04–0.05-ms duration. Current was set at 1.5–2.0-fold that of threshold for evoking VPm responses. Thresholds were tested at the beginning of each recording session. Medial lemniscus stimulation consisted of 1 Hz cathodal 40–80-μA pulses of 0.03–0.05-ms duration, also at 1.5–2.0-fold that of threshold. In some recording sessions, paired-pulse stimulation (inter-pulse interval, 25 ms) was used. During a recording session, electrical stimuli were presented continually; whisking and nonwhisking epochs were selected for off-line analyses. We did not observe any disturbance of the rats' behavior as a result of either whisker follicle or medial lemniscus microstimulation.

**SpVi inactivation.** An implanted stainless steel cannula (outer diameter, 0.042 inches; inner diameter, 0.033 inches) targeted the interpolaris subdivision of the SpVi. The SpVi was located stereotaxically (13–14 mm caudal to bregma, 3.2–3.6 mm from midline, depth of 6.5–7.0 mm) and confirmed by physiological recordings. The cannula was used to infuse 8–10 μl of bupivacaine (5 mg $ml^{-1}$, Hospira) using a syringe pump (0.8 μL $min^{-1}$). Data collection began 5 min after termination of drug infusion. We did not record data after drug washout because of the long recovery time and water satiation of the rat.

**Electrophysiological recordings and data analysis.** EMG and VPm signals were recorded using custom-made head-stage amplifiers. EMG signals, filtered at 0.3–3 kHz, were digitized at 10 kHz and saved on computer disk. The VPm signal was first bandpass filtered at 1 and 10k Hz. LFP signals were further filtered at 1–500 Hz and MUA recordings at 0.3–10 kHz.

LFP and MUA data were analyzed separately for whisking and nonwhisking epochs. Whisking-in-air typically consisted of relatively large amplitude sweeps at 5–10 Hz, but we also included periods when whisking was smaller in amplitude but still characterized by rhythmic protractions and retractions. We did not attempt to correlate VPm activity with detailed whisking kinematics. An epoch was classified as nonwhisking when there were no observable whisker movements and no rhythmic EMG activity (**Supplementary Fig. 7**). Epochs that were associated with incidental contact of whiskers with the platform were excluded.

Individual recording sessions yielded 100–300 stimulus presentations for each condition (whisking and nonwhisking). For LFPs, evoked responses were averaged across stimuli and trials. With whisker follicle stimulation, we identified the VPm response on the basis of its latency and similarity in shape to LFPs that were evoked by whisker deflections in lightly sedated animals[20]. The VPm LFP has an abrupt positive-to-negative transition during which MUA spiking occurred (**Fig. 4a,b**). Whisker follicle stimulation also evoked an immediately preceding triphasic potential that varied from animal to animal and that may reflect highly synchronous spiking activity in incoming trigeminothalamic fibers from PrV; we did not analyze this early potential because of uncertainty as to its origin. LFPs evoked by whisker deflections can be well quantified by peak magnitude, slope or the area under the curve of negativity[20]. We measured the amplitude of the VPm component of the whisker follicle– or

medial lemniscus–evoked LFP from the nadir of the negativity to the onset of the preceding positive-to-negative transition (**Fig. 4a**). Stimulus-averaged responses were examined to identify these time points, which were also used for computing mean and variance values on a stimulus-by-stimulus basis. For MUA, spike occurrences were accumulated into PSTHs with 0.1-ms bins.

Because several days often intervened between recording sessions, it was sometimes necessary to reinsert the whisker follicle–stimulating wires. Data were therefore analyzed separately for each recording session. We compared data obtained in whisking and nonwhisking epochs during individual recording sessions. Mann-Whitney tests were used for comparing whisking versus nonwhisking data within individual sessions. Wilcoxon signed-rank tests were used for group data.

After the final recording session for each animal, an electrolytic lesion was made through the VPm (and medial lemniscus) microelectrode. The rat was deeply anesthetized with pentobarbital sodium (100 mg per kg, intraperitoneal) and perfused as above. Recording and stimulating sites were identified histologically and confirmed as being in VPm or medial lemniscus. In rats having an implanted cannula, the brainstem was similarly examined to visualize its track and termination point.

*Note: Supplementary information is available on the Nature Neuroscience website.*

**ACKNOWLEDGMENTS**

We thank H. Kyriazi and T. Prigg for excellent technical assistance, and E. Merriam for helpful comments on the manuscript. This work was supported by US National Institutes of Health grants NS19950 and NS58758.

**AUTHOR CONTRIBUTIONS**

S.L., G.E.C. and D.J.S. designed the experiments. S.L. conducted the experiments. S.L., G.E.C. and D.J.S. analyzed data. G.E.C. and D.J.S. supervised the project. S.L., G.E.C. and D.J.S. wrote the manuscript.

Published online at http://www.nature.com/natureneuroscience/
Reprints and permissions information is available online at http://npg.nature.com/reprintsandpermissions/

1. Ahissar, E. & Kleinfeld, D. Closed-loop neuronal computations: focus on vibrissa somatosensation in rat. *Cereb. Cortex* **13**, 53–62 (2003).
2. Carvell, G.E., Miller, S.A. & Simons, D.J. The relationship of vibrissal motor cortex unit activity to whisking in the awake rat. *Somatosens. Mot. Res.* **13**, 115–127 (1996).
3. Fanselow, E.E. & Nicolelis, M.A. Behavioral modulation of tactile responses in the rat somatosensory system. *J. Neurosci.* **19**, 7603–7616 (1999).
4. Krupa, D.J., Wiest, M.C., Shuler, M.G., Laubach, M. & Nicolelis, M.A. Layer-specific somatosensory cortical activation during active tactile discrimination. *Science* **304**, 1989–1992 (2004).
5. Hentschke, H., Haiss, F. & Schwarz, C. Central signals rapidly switch tactile processing in rat barrel cortex during whisker movements. *Cereb. Cortex* **16**, 1142–1156 (2006).
6. Ferezou, I. *et al.* Spatiotemporal dynamics of cortical sensorimotor integration in behaving mice. *Neuron* **56**, 907–923 (2007).
7. Crochet, S. & Petersen, C.C. Correlating whisker behavior with membrane potential in barrel cortex of awake mice. *Nat. Neurosci.* **9**, 608–610 (2006).
8. Miyashita, E., Keller, A. & Asanuma, H. Input-output organization of the rat vibrissal motor cortex. *Exp. Brain Res.* **99**, 223–232 (1994).
9. Zhang, Z.W. & Deschenes, M. Projections to layer VI of the posteromedial barrel field in the rat: a reappraisal of the role of corticothalamic pathways. *Cereb. Cortex* **8**, 428–436 (1998).
10. Sillito, A.M. & Jones, H.E. Corticothalamic interactions in the transfer of visual information. *Phil. Trans. R. Soc. Lond. B* **357**, 1739–1752 (2002).
11. Alitto, H.J. & Usrey, W.M. Corticothalamic feedback and sensory processing. *Curr. Opin. Neurobiol.* **13**, 440–445 (2003).
12. Landry, P. & Dykes, R.W. Identification of two populations of corticothalamic neurons in cat primary somatosensory cortex. *Exp. Brain Res.* **60**, 289–298 (1985).
13. Kelly, M.K., Carvell, G.E., Hartings, J.A. & Simons, D.J. Axonal conduction properties of antidromically identified neurons in rat barrel cortex. *Somatosens. Mot. Res.* **18**, 202–210 (2001).
14. Swadlow, H.A. Efferent neurons and suspected interneurons in S-1 vibrissa cortex of the awake rabbit: receptive fields and axonal properties. *J. Neurophysiol.* **62**, 288–308 (1989).
15. Swadlow, H.A. & Hicks, T.P. Somatosensory cortical efferent neurons of the awake rabbit: latencies to activation via supra- and subthreshold receptive fields. *J. Neurophysiol.* **75**, 1753–1759 (1996).
16. Beloozerova, I.N. *et al.* Activity of different classes of neurons of the motor cortex during postural corrections. *J. Neurosci.* **23**, 7844–7853 (2003).
17. Sirota, M.G., Swadlow, H.A. & Beloozerova, I.N. Three channels of corticothalamic communication during locomotion. *J. Neurosci.* **25**, 5915–5925 (2005).
18. Temereanca, S. & Simons, D.J. Functional topography of corticothalamic feedback enhances thalamic spatial response tuning in the somatosensory whisker/barrel system. *Neuron* **41**, 639–651 (2004).
19. Land, P.W., Buffer, S.A. Jr & Yaskosky, J.D. Barreloids in adult rat thalamus: three dimensional architecture and relationship to somatosensory cortical barrels. *J. Comp. Neurol.* **355**, 573–588 (1995).
20. Temereanca, S. & Simons, D.J. Local field potentials and the encoding of whisker deflections by population firing sychrony in thalamic barreloids. *J. Neurophysiol.* **89**, 2137–2145 (2003).
21. Castro-Alamancos, M.A. Different temporal processing of sensory inputs in the rat thalamus during quiescent and information processing states *in vivo*. *J. Physiol. (Lond.)* **539**, 567–578 (2002).
22. Jacquin, M.F., Golden, J. & Rhoades, R.W. Structure-function relationships in rat brainstem subnucleus interpolaris. III. Local circuit neurons. *J. Comp. Neurol.* **282**, 24–44 (1989).
23. Furuta, T. *et al.* Inhibitory gating of vibrissal inputs in the brainstem. *J. Neurosci.* **28**, 1789–1797 (2008).
24. Hattox, A., Li, Y. & Keller, A. Serotonin regulates rhythmic whisking. *Neuron* **39**, 343–352 (2003).
25. Cramer, N.P. & Keller, A. Cortical control of a whisking central pattern generator. *J. Neurophysiol.* **96**, 209–217 (2006).
26. Jones, E.G. & Powell, T.P. An electron microscopic study of the mode of termination of cortico-thalamic fibres within the sensory relay nuclei of the thalamus. *Proc. R. Soc. Lond. B* **172**, 173–185 (1969).
27. Liu, X.B., Honda, C.N. & Jones, E.G. Distribution of four types of synapse on physiologically identified relay neurons in the ventral posterior thalamic nucleus of the cat. *J. Comp. Neurol.* **352**, 69–91 (1995).
28. Erisir, A., Van Horn, S.C. & Sherman, S.M. Relative numbers of cortical and brainstem inputs to the lateral geniculate nucleus. *Proc. Natl. Acad. Sci. USA* **94**, 1517–1520 (1997).
29. Diamond, M.E., Armstrong-James, M., Budway, M.J. & Ebner, F.F. Somatic sensory responses in the rostral sector of the posteriorgroup (POm) and in the ventral posterior medial nucleus (VPM) of the rat thalamus: dependence on the barrel field cortex. *J. Comp. Neurol.* **319**, 66–84 (1992).
30. Ghazanfar, A.A., Krupa, D.J. & Nicolelis, M.A. Role of cortical feedback in the receptive field structure and nonlinear response properties of somatosensory thalamic neurons. *Exp. Brain Res.* **141**, 88–100 (2001).
31. Yuan, B., Morrow, T.J. & Casey, K.L. Responsiveness of ventrobasal thalamic neurons after suppression of SI cortex in the anesthetized rat. *J. Neurosci.* **5**, 2971–2978 (1985).
32. Yuan, B., Morrow, T.J. & Casey, K.L. Corticofugal influences of S1 cortex on ventrobasal thalamic neurons in awake rat. *J. Neurosci.* **6**, 3611–3617 (1986).
33. White, E.L. & Keller, A. Intrinsic circuitry involving the local axon collaterals of corticothalamic projection cells in mouse SmI cortex. *J. Comp. Neurol.* **262**, 13–26 (1987).
34. Urbain, N. & Deschênes, M. A new thalamic pathway of vibrissal information modulated by the motor cortex. *J. Neurosci.* **27**, 12407–12412 (2007).
35. Ghez, C. & Pisa, M. Inhibition of afferent transmission in cuneate nucleus during voluntary movement in the cat. *Brain Res.* **40**, 145–155 (1972).
36. Coulter, J.D. Sensory transmission through lemniscal pathway during voluntary movement in the cat. *J. Neurophysiol.* **37**, 831–845 (1974).
37. Seki, K., Perlmutter, S.I. & Fetz, E.E. Sensory input to primate spinal cord is presynaptically inhibited during voluntary movement. *Nat. Neurosci.* **6**, 1309–1316 (2003).
38. Furuta, T., Nakamura, K. & Deschenes, M. Angular tuning bias of vibrissa-responsive cells in the paralemniscal pathway. *J. Neurosci.* **26**, 10548–10557 (2006).
39. Leiser, S.C. & Moxon, K.A. Responses of trigeminal ganglion neurons during natural whisking behaviors in the awake rat. *Neuron* **53**, 117–133 (2007).
40. Urbain, N. & Deschenes, M. Motor cortex gates vibrissal responses in a thalamocortical projection pathway. *Neuron* **56**, 714–725 (2007).
41. Hall, R.D. & Lindholm, E.P. Organization of motor and somatosensory neocortex in the albino rat. *Brain Res.* **66**, 23–38 (1974).
42. Hoffer, Z.S., Hoover, J.E. & Alloway, K.D. Sensorimotor corticocortical projections from rat barrel cortex have an anisotropic organization that facilitates integration of inputs from whiskers in the same row. *J. Comp. Neurol.* **466**, 525–544 (2003).
43. Donoghue, J.P. & Wise, S.P. The motor cortex of the rat: cytoarchitecture and microstimulation mapping. *J. Comp. Neurol.* **212**, 76–88 (1982).
44. Haiss, F. & Schwarz, C. Spatial segregation of different modes of movement control in the whisker representation of rat primary motor cortex. *J. Neurosci.* **25**, 1579–1587 (2005).
45. Kakei, S., Hoffman, D.S. & Strick, P.L. Muscle and movement representations in the primary motor cortex. *Science* **285**, 2136–2139 (1999).
46. Graziano, M. The organization of behavioral repertoire in motor cortex. *Annu. Rev. Neurosci.* **29**, 105–134 (2006).
47. Welker, W.I. Analysis of sniffing of the albino rat. *Behaviour* **22**, 223–244 (1964).
48. Carvell, G.E. & Simons, D.J. Biometric analyses of vibrissal tactile discrimination in the rat. *J. Neurosci.* **10**, 2638–2648 (1990).
49. Towal, R.B. & Hartmann, M.J. Right-left asymmetries in the whisking behavior of rats anticipate head movements. *J. Neurosci.* **26**, 8838–8846 (2006).
50. Simons, D.J. & Carvell, G.E. Thalamocortical response transformation in the rat vibrissa/barrel system. *J. Neurophysiol.* **61**, 311–330 (1989).